

Integrated Thermopile Sensors*

A. W. VAN HERWAARDEN

Sensor Integration, P.O. Box 3233, Delft (The Netherlands)

D. C. VAN DUYN and B. W. VAN OUDHEUSDEN

Electrical Engineering Department, Delft University of Technology, Delft (The Netherlands)

P. M. SARRO

DIMES, Delft University of Technology, Delft (The Netherlands)

Abstract

This paper is about integrated silicon thermopiles and their applications in silicon sensors. After a short description of the thermoelectric effect and its use in silicon thermopiles, some attention is devoted to the design of micromachined structures for implementing thermal sensors. The various sensing principles based on thermal effects are discussed next. Finally, an impression is given of some of the recently developed silicon-thermopile sensors which implement these sensing principles.

Introduction

The last ten years have seen significant advances in the development of integrated silicon thermopiles, devices that measure temperature differences in a silicon chip. The integrated thermopile is based on the same transduction principle as the thermocouple: the Seebeck effect [1, 2]. The typical structure consists of p-type silicon strips in an n-type epilayer or well, interconnected by aluminum strips. By connecting many strips a large sensitivity is obtained (see Fig. 1).

Thermopiles have various attractive properties compared with the other sensors which are frequently used for temperature-difference measurement, such as the transistor pair and the resistance bridge. First, the thermopile is based on the self-generating Seebeck effect, in which the input signal supplies the power for the output signal. This ensures that:

- the thermopile has an output signal without offset and offset drift, because there cannot be any output signal without input power;
- the thermopile does not suffer from interference from any physical or chemical signals except light (which can easily be shielded) because the Seebeck effect and the photoelectric effect are the only two self-generating effects in silicon;

- the thermopile does not need any biasing;
- the read-out is very simple, only a voltmeter is required;
- there is no interference caused by power supplies.

Secondly, the Seebeck effect in silicon is rather large, 0.5–1 mV/K per strip and, in general, many strips can be connected in parallel. Moreover, the sensitivity of the thermopile is hardly influenced by variations in the electrical parameters across the wafer or by the temperature. With transistors and resistors, both the sensitivity and the offset usually depend on the position on the wafer and on the temperature.

Finally, the thermopile fabrication process is fully compatible with both standard bipolar and CMOS processes (allowing on-sensor electronics), and the so-called electrochemically controlled etching techniques used to increase the sensitivity of thermopile sensors [3]. In contrast, transistors needing isolation diffusions cannot be used in etched structures because this etching technique relies on the substrate–epilayer p–n junction.

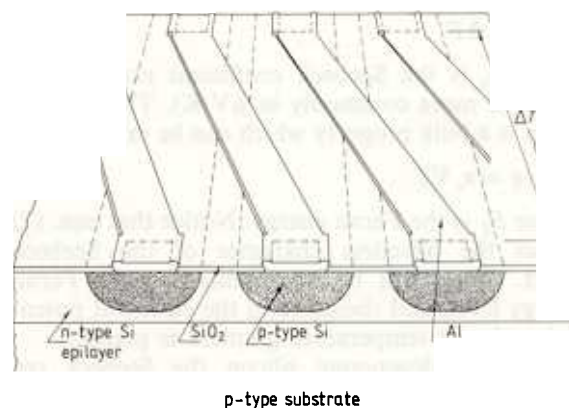


Fig. 1. An integrated p-type silicon/aluminum thermopile.

*Invited paper.

The integrated thermopile also has some disadvantages compared to transistor pairs and resistance bridges. Its nature requires a silicon connection between the hot and reference parts of the sensor, in which the thermopile is integrated. This limits the thermal resistance of the sensor. Also, the internal electrical resistance of the thermopile can be rather high if many strips are used to obtain sufficient sensitivity. However, in most cases the better quality of the output signal of the thermopile will outweigh this disadvantage.

In this paper we briefly discuss the characteristics of the Seebeck effect. We also shed some light on the optimum choice of structure for each sensor. To enhance the sensitivity of thermopile sensors, etching techniques are used [3], and basically three different structures have emerged for various applications: the closed-membrane structure; the cantilever-beam structure; and the floating-membrane structure. For each sensor and each application, a well-founded choice must be made. The various thermal sensing principles to which thermopiles can be applied will also be discussed, some of which show more potential than others at the moment. Finally, we describe the various thermopile sensors that have been developed over the past few years, showing quite some progress, especially for infrared sensors, flow sensors, vacuum sensors and thermal converters [4–7].

The Seebeck Effect

In the case that two semiconductors 'a' and 'b' are joined together at the hot point and a temperature difference ΔT is maintained between this point and the cold point (see Fig. 2), an open circuit voltage ΔV is developed between the leads at the cold point. This effect was called the Seebeck effect in honor of its discoverer, the German T. J. Seebeck (1770–1831), and can be expressed by

$$\Delta V = \alpha_s \Delta T \quad (1)$$

where α_s is the Seebeck coefficient expressed in V/K (or more commonly in $\mu\text{V}/\text{K}$). The Seebeck effect is a bulk property which can be expressed as

$$\nabla E_F / q = \alpha_s \nabla T \quad (2)$$

where E_F is the Fermi energy. Notice that eqn. (2) shows the offsetless character of the Seebeck effect. There will be no gradient in the Fermi energy level, and therefore in the electrical potential, unless a temperature gradient is present.

For non-degenerate silicon the Seebeck coefficient may be approximated by using simple Maxwell–Boltzmann statistics. Three main effects are present. First, with increasing temperature the

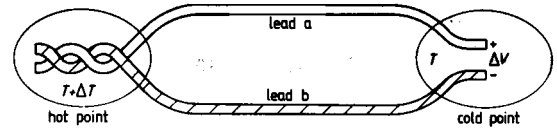


Fig. 2. The Seebeck effect: an electrical voltage ΔV due to a temperature difference ΔT .

silicon becomes more intrinsic. Secondly, with increasing temperature the charge carriers have a higher average velocity, leading to charge build-up on the cold side of the silicon. Moreover, the scattering of charge carriers is usually energy (and thus temperature) dependent, likewise leading to charge build-up on the cold or hot side of the silicon, depending on whether the hot carriers can move more freely than the cold carriers or are 'trapped' by increased scattering. Finally, the temperature difference in the silicon causes a net flow of phonons from hot to cold. In a certain temperature region (10–500 K) and for non-degenerate silicon, a transfer of momentum from acoustic phonons to the charge carriers can occur. As there is a net phonon momentum directed from hot to cold, this will drag the charge carriers towards the cold side of the silicon. In sum, the total Seebeck coefficient in non-degenerate n-type silicon is approximated by

$$\alpha_s = -\frac{k}{q} \{ \ln(N_c/n) + 2.5 + s_n + \varphi_n \} \quad (3)$$

with q as the elementary charge, k as the Boltzmann constant, N_c as the conduction-band density of states and n the electron density (fixed by the doping concentration). The factor s_n is the exponent in the exponential relation between the mean-free-time between collisions and the energy, which is typically of the order from -1 to 2 . The phonon-drag effect is represented by φ_n , and it ranges from 0 for highly-doped silicon to 5 for low-doped silicon at room temperature. For p-type silicon a similar expression is found, except that the coefficient is now positive.

For practical sensor design-purposes it is very convenient to approximate the Seebeck coefficient as a function of electrical resistivity

$$\alpha_s = \frac{mk}{q} \ln(\rho/\rho_o) \quad (4)$$

with $\rho_o \approx 5 \times 10^{-6} \Omega \text{ m}$ ($5 \times 10^{-4} \Omega \text{ cm}$) and $m \approx 2.6$ as constants [1] (see Fig. 3). Typical values of the Seebeck coefficient of silicon are 500 – $700 \mu\text{V}/\text{K}$ for the optimum compromise between low resistance and high Seebeck coefficient [1].

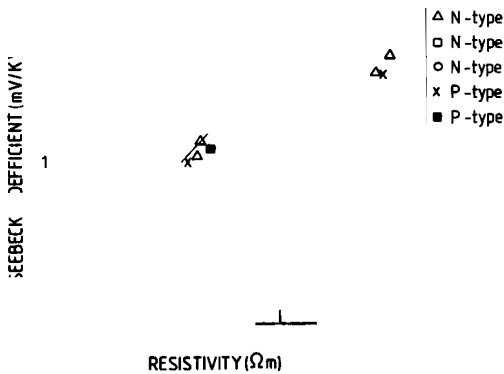


Fig. 3. The Seebeck coefficient of monocrystalline silicon at 300 K versus electrical resistivity (symbols, experimental results; dashed line, results calculated from eqn. (4)).

The Peltier Effect

Apart from the Seebeck effect, yet another important thermoelectric offset exists: the Peltier effect. It is heat absorption from or release to the ambient, when an electrical current flows through the junction of two different materials. The Peltier effect is reversible, since heat is absorbed or released depending on the direction of the current. The Peltier coefficient Π (in V) which quantifies the ratio of heat absorption to electrical current, is equal to the Seebeck coefficient times the absolute temperature, called the first Kelvin relation

$$\Pi = \alpha_s T \tag{5}$$

Care should be taken when designing thermal devices using heating resistors, otherwise the Peltier effect may give rise to considerable asymmetries. A common value for the Peltier coefficient is 100–300 mV, which is significant if heating voltages of, for instance, 1–3 V are used. In such cases a Peltier heat flow of 10% of the generated (irreversible) Joule heat will flow from one contact to the other.

Thermopiles

Based on the Seebeck effect, integrated silicon thermopiles have been fabricated, in which many p-type silicon–aluminum thermocouples are placed next to each other, experiencing the same temperature gradient. By connecting the plus-pole of the first couple to the minus-pole of the second, and so on, the thermoelectric voltages are added to give a high sensitivity, see Fig. 1. In practice, sensitivities of 5–50 mV/K are common, depending on the sensor structure. A parameter of importance is the desired electrical resistance of the thermopile, which is mainly determined by

the number of strips, the length of the strip in squares (length–width ratio), and the electrical sheet resistance [1]. Resistances of the order of 10–100 k Ω are in practice high enough to allow for a high sensitivity, while low enough to avoid too much interference.

Thermal-sensor Structures

There are two ways to employ the integrated thermopiles. One can simply integrate a silicon thermopile and use the sensor chip to detect temperature differences inside or outside the sensor chip. Unfortunately, silicon is a very good heat conductor, and the 500 μm silicon substrate underneath the 5 μm thick thermopile spoils the sensitivity with a thermal short-circuit. It turns out to be very rewarding to remove this silicon by means of micromachining of silicon [3]. By creating a membrane of only 5–10 μm thickness, the thermal resistance of the sensor is increased by two orders of magnitude, without degradation of electrical properties (Fig. 4). The sensitivity of the sensor, which is directly proportional to its thermal resistance is, therefore, also increased by two orders of magnitude.

Several structures can be made in which a ‘cold’ and a ‘hot’ region are separated by means of micromachining of silicon. The link between the hot and cold region is formed by a silicon membrane or cantilever beam, which contains the thermopile. The heat generated or absorbed in some manner in the hot region flows through the silicon membrane or cantilever beam to the cold region, usually at ambient temperature, causing a temperature difference across the thermal resistance of the membrane or cantilever beam. The following drawings and explanations will clarify the various possibilities.

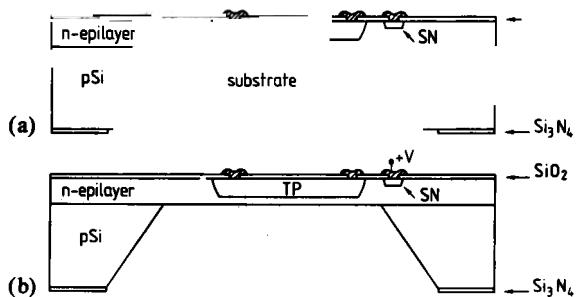
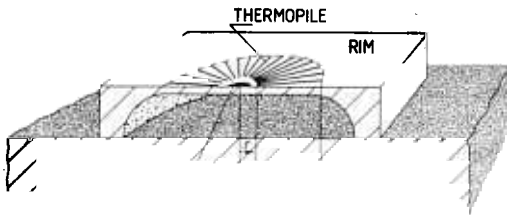


Fig. 4. (a) Wafer-thick sensor with 500 μm substrate thermally short-circuiting the thermopile (TP); (b) micromachined sensor with a 5- μm -thick membrane, giving 100 times higher thermal resistance and sensitivity.



Closed Membrane

The structure with the lowest thermal resistance between the hot and cold regions is the closed membrane, see Fig. 5. The cold region, containing the cold junctions of the thermopile, is formed by a wafer-thick rim around the etched membrane. This rim serves not only as heat sink, but also as suspension of the etched structure, mechanical protection, and a convenient means of handling the sensor. The hot region is in fact the membrane area within the radius of the hot junctions of the thermopile. Because the thermal resistance is given by the logarithm of the inner and outer radius of the thermopile junctions, thermal resistances are practically limited to $0.5 \times R_{st}$, where R_{st} is the thermal sheet resistance of the membrane. For a monocrystalline silicon membrane of $7 \mu\text{m}$ thickness, $R_{st} = 1000 \text{ K/W}$. This structure is characterized by a low thermal resistance, a small time constant and a thermopile with the highest sensitivity.

Cantilever Beam

The thermal resistance of the cantilever beam is given by the thermal sheet resistance times the length-width ratio L/W of the cantilever beam. The resistance can be made substantially larger than that of a closed membrane, because the length-width ratio can be made much larger than

0.5; values of 5 are not uncommon, see Fig. 6. There is yet another (thermal) advantage to this structure over the closed membrane: the hot region beyond the thermopile can be made rather large. In the case of the closed membrane, only a small circle at the center is available as a hot region, where a piece of cantilever beam with width W and, in theory, unlimited length can be used. Mechanically, the cantilever beam is more fragile than the closed membrane, which can be a disadvantage during both production and use. This structure is characterized by a medium thermal resistance, medium time constant and medium thermopile sensitivity.

A special case of cantilever beam is the bridge in which two cantilever beams are joined at the tips. If the bridge has a length L and a width W , then its thermal resistance is $0.25 \times R_{st} \times L/W$. This is exactly one quarter of the thermal resistance of a cantilever beam of the same dimensions because, in this case, two cantilever beams of half the length are put in parallel. This structure has a slightly lower thermal resistance and time constant than the cantilever beam, at a higher thermopile sensitivity.

Floating Membrane

In this structure a large piece of the membrane is etched free from the rim, hanging only by a few suspension beams, see Fig. 7. In the suspension beams thermopiles measure the temperature difference between the 'floating' membrane and the rim at ambient temperature. In this structure a very large hot area is achieved, with also a very high thermal resistance, because the suspension beams are usually made very narrow and long. Consequently, not many strips can be accommodated by the suspension beams, which leads to a low thermopile sensitivity. Nevertheless, because of the very high thermal resistance, a high overall sensitivity is obtained. Large time constants result from this set-up. This structure is much more

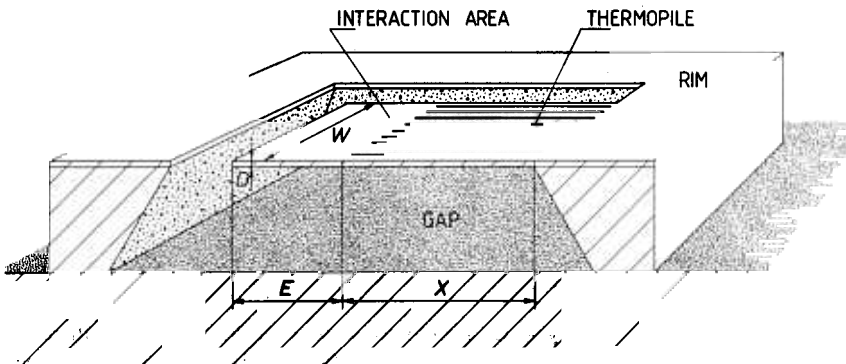


Fig. 6. Cantilever-beam structure with thermopile length X and width W , and hot region beyond the thermopile of length E .

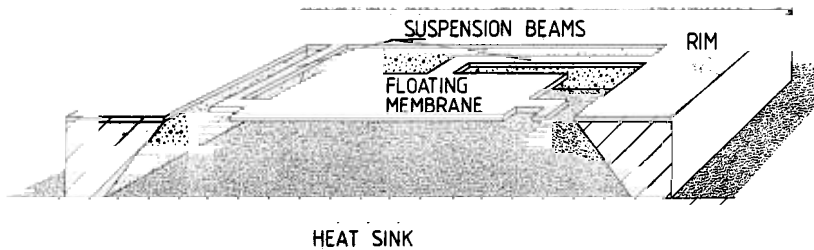


Fig. 7. Floating-membrane structure with a large floating membrane, suspended from the wafer-thick rim by four narrow, long cantilever beams.

fragile than the other structures, not only in use, but also in production. Special care should be taken to avoid critical designs from a mechanical point of view. The floating membrane has the highest thermal resistance and time constant, and the lowest thermopile sensitivity.

Thermal Sensing Principles

There are various ways in which integrated thermopiles can be put to work. A short list of the various sensing principles relying on temperature-difference measurement will be given [8–12]. In some principles we measure thermal signals originating from outside the sensor chip. This leads to various practical problems. Attention has therefore been focused on sensing principles, in which the thermal signal is generated within the sensor by another physical signal. This results in the so-called tandem transducers where an output of the electrical type is obtained via the thermal signal domain. Moreover, these tandem transducers also allow micromachining, given them extra sensitivity.

Direct Measurement Principles

Temperature-difference measurement

One obvious application of the integrated thermopile would be the measurement of temperature differences existing in the ambient with a silicon chip containing a thermopile. However, silicon is a very good heat conductor, and the thermal contact resistances will in many cases be of significant size, compared with the thermal resistance of the sensor. This will then lead to inaccurate measurements.

Heat-flux measurement

Another application is using the thermopile chip for the measurement of heat flux in the ambient, placing the chip in the circuit in which the heat flows. If the source has a good output

(thermal) resistance, an accurate measurement should be feasible. However, the problem of connecting the sensor thermally to the heat source and sink, and electrically to the outside, remains. In addition, the signal which is eventually measured is the temperature difference, so that a conversion is made with the thermal resistance of the sensor as parameter.

Other thermal signals

The thermopile can also be used to determine other thermal signals in the ambient, such as thermal conductivity. Again some way of converting the thermal signal into a temperature difference needs to be found, and signals existing outside of the sensor chip are difficult to measure, for practical purposes.

Tandem-transduction Principles

Sensors in which an on-chip temperature difference is created avoid this problem and, moreover, allow for micromachined structures, which are two orders of magnitude more sensitive than wafer-thick sensors. The various thermal-sensing principles satisfying the on-chip temperature-difference requirement are given below.

True r.m.s. measurement

In this measurement method, the true r.m.s. (root-mean-square) value of an electrical a.c. voltage (or current) is determined by measuring the power in the signal. First the signal is put across (or led through) a heating resistor located in the hot region of a micromachined structure. The resulting temperature difference is measured by a thermopile. Then a d.c. signal is put across (or led through) the same resistor, and adjusted to give the same output in the thermopile. The true r.m.s. value of the a.c. signal equals that of the d.c. signal (which is simply the d.c. voltage or current) when equal amounts of heat are dissipated. Because no area for interaction with the ambient is required, all three structures mentioned

above can be used for the true r.m.s. converter, depending on the circumstances. Excellent results have been accomplished with closed membranes [7].

Infrared detection

One of the most elegant thermal sensing methods is the thermal infrared-radiation detection. It is a fully offsetless method, because both transduction steps, from infrared to heat and the thermopile transduction, are self-generating. The principle can very easily be implemented in a thermopile infrared sensor. In the hot region of the sensor a black infrared-radiation absorbing coating is applied. This will absorb the radiation and transduce it into heat. The heat will cause temperature differences across the thermopile, which thus gives an output proportional to the incident infrared radiation. Because in the infrared sensor the largest possible interaction area with the ambient is desired, cantilever beams or floating membranes are the best choice. Using floating membranes, one should take care not to make the thermal resistance to the ambient too high.

Flow measurement

The fluid-flow sensors (fluid is either gas or liquid) rely on the principle that thermal conductance from the hot to the cold regions, as determined by silicon cantilever beams or membranes, is lowered by a thermal conductance to the ambient (= the cold region) parallel to the thermal conductance through the silicon. This thermal conductance is heat transfer to a fluid flow. Because the size of the heat transfer is related to the fluid flow velocity, the effective thermal resistance between hot and cold regions of flow sensors is dependent on the flow velocity. This thermal resistance is measured by dissipating power in a heating resistor in the hot region. The resulting temperature difference is proportional to the effective thermal resistance. Thus, also the sensor output is dependent upon fluid flow velocity.

When measuring gas flows, cantilever beams or floating membranes are preferable, because of their higher thermal resistance. In the case of liquid flows, there is no need for a high thermal resistance and a closed membrane may be preferred because it allows separation between the liquid flow and the electrical parts of the sensor.

Vacuum gauging

The thermal vacuum sensing principle is used in the integrated vacuum sensor, which is closely related to the traditional thermocouple gauge and the Pirani gauge. The vacuum sensor measures absolute gas pressures up to approximately 1 atm.

It relies on the decrease in effective thermal resistance between the hot and cold regions of the sensor, caused by thermal conductance by gas molecules. Up to a certain pressure, this conductance is proportional to pressure, causing the pressure dependence of the effective thermal resistance in the sensor. By heating the hot region and measuring the resulting temperature increase, this thermal resistance and the pressure is determined. For the vacuum sensor, a floating membrane structure gives the best sensitivity and resolution.

Fluid level detection

Thermal fluid-level detection is a third principle in which the effective thermal resistance between hot and cold regions is influenced by an unknown parameter. Just as with the flow and vacuum sensing principles, the presence of a fluid provides alternative thermal conduction paths for the heat, decreasing the temperature when heating with a constant power. So, fluid-level detectors will sense whether or not they are immersed in a fluid with a thermal conductivity different from that of their usual environment. Actually, it does not matter whether that usual environment is air, another gas, or even a liquid with a higher thermal conductivity, the only factor of importance is the difference in thermal conductivities of the two media. For this sensor the same reasoning for choosing the structure applies as for the flow sensor.

Fluid type/mixture sensing

The principle of the vacuum sensor or fluid-level detector can also be used to detect the type of gas or liquid, if two fluids with different thermal conductivities have to be distinguished. The different thermal conductivities parallel to the thermal resistance of the silicon cantilever beams or membranes will cause distinctly different output signals in heated sensors, depending on the fluid type surrounding the sensor. It is also possible to determine the relative proportions of a mixture of two fluids, by first calibrating the output signal of a sensor as a function of the relative proportions. Also for this sensor the same reasoning for choosing the structure applies as for the flow sensor.

Microcalorimetry

This sensing principle resembles that of the infrared sensor, in that it is an offsetless, self-generating sensing principle. Here the hot region of the calorimeter is coated with a chemical-reaction catalyst instead of a black layer. In the presence of the particular substances which react under the influence of the catalyst, the heat of the catalytic reaction will now cause a temperature

difference across the thermopile, and result in an output signal proportional to the rate of reaction. Of course, instead of a chemical catalyst, other coatings can be applied to the hot region of the sensor, making it sensitive to other physical signals. Middelhoek suggested the application of a coating which converts microwaves into heat, thus making a very simple and easy to use microwave sensor [13]. Another example would be a ferromagnetic coating with high hysteresis, in which a.c. magnetic fields would cause much heat generation. Again, also for this sensor, the same reasoning for choosing the structure applies as for the flow sensor.

Psychrometry

The last example of a thermal sensing principle is given by the psychrometer, which measures the relative humidity of air (or another gas). It consists of two parts, neither of which is heated. The air is blown with high velocity past the parts. The first part measures the temperature of the air. The second part is kept wet with water. This water will evaporate into the air stream, and the rate of evaporation increases when the relative humidity of the air is lower. The evaporation process will cool the second part, making its 'hot' area colder than ambient. With increasing evaporation, the cooling is stronger, therefore the temperature difference between the dry and the wet part is a measure of the relative humidity. The need for keeping one part wet and to blow the air with great velocity past the sensor (10 m/s), in combination with the very nonlinear, temperature dependent response of the sensor, makes this sensor rather impractical.

Examples of Successful Thermopile-sensor Implementations

True r.m.s. Converters

The true r.m.s. converter is a device which measures the root-mean-square value of alternating electrical signals, such as currents and voltages. The idea is that the device first squares the a.c. signal, then takes the average, and determines the root of this average. This is the only way to determine the power content of a signal independent of the signal shape, i.e., be it a sinusoidal shape, a block wave, or any other shape.

There are various ways in which true r.m.s. converters can be implemented. Electronic versions have been made in which, for instance, translinear circuits provide the quadratic conversion. The most accurate versions, however, are of the thermal type, in which heat is dissipated by putting an a.c. voltage across a heat resistor. The

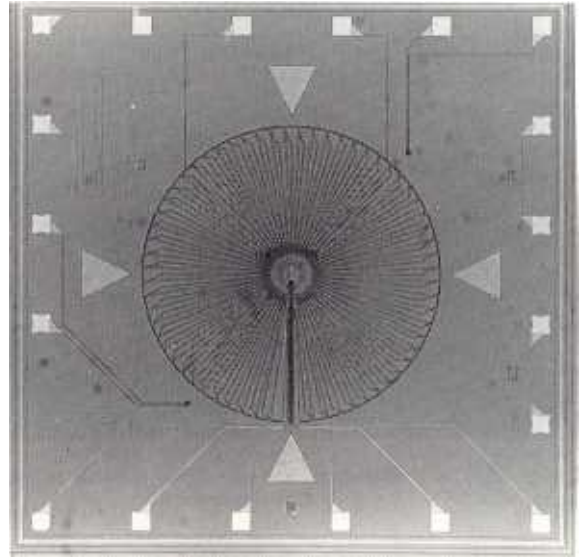


Fig. 8. True r.m.s. converter based on an integrated-silicon thermopile incorporated in a closed membrane.

dissipation action is quadratic by nature and averages because of the large thermal time constants. This makes the thermal conversion very accurate up to high frequencies. The primary standards are usually vacuum tubes with a single resistance wire, and a thermocouple attached to it. Transfer accuracies better than 1 ppm over a frequency range of hundreds of MHz can be obtained.

Kerkhoff and Meijer have fabricated thermal converters in silicon using wafer-thick samples and integrated silicon thermopiles to measure the amplitude of a.c. signals [14]. Hochstenbach, in cooperation with NV, Philips Gloeilampenfabrieken, The Netherlands, has made a first prototype true r.m.s. converter using integrated silicon thermopiles in a closed-membrane structure (see Fig. 8). This device obtained a bandwidth of 0.5 GHz, and a certified low-frequency a.c./d.c. transfer better than 100 ppm [7, 15].

Infrared Sensors

Considerable effort has been devoted to the development of integrated thermopile infrared sensors. Sensors with various shapes have been implanted and tested, including cantilever-beam sensors and arrays (see Fig. 9), and floating-membrane sensors and arrays [16–18]. It turns out that, especially with floating-membrane structures, quite sensitive infrared detectors can be made. Sensitivities of tens of volts per watt are attainable, at time constants of the order of tens to hundreds of milliseconds. The encapsulation gas in the infrared sensor will diminish the sensitivity strongly in the case of a floating-membrane

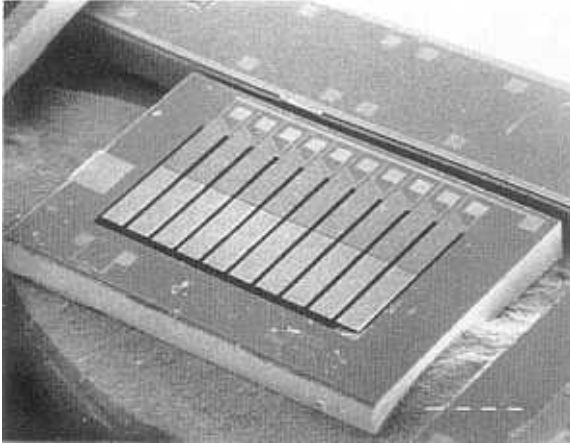


Fig. 9. SEM of a 10-element cantilever-beam infrared sensor array, with $2.6 \times 1.8 \text{ mm}^2$ overall dimensions.

structure, for the same reason that makes this structure such a very good vacuum sensor. This sets a limit to the sensitivity that can be attained in practice, even when using low-conductive encapsulation gases such as argon.

An interesting feature of integrated-thermopile infrared sensors is that it is very easy to make arrays with these devices within one rim, so that no silicon area is wasted on separation between the array elements. By combining a sensor like the one shown in Fig. 9 with a circular Fresnel Zone Plate [18], Sarro *et al.* have made a monochromatic detector. Radiation in the (visible) wavelength range of 497 and 488 nm was detected by beams separated by three intermediate beams, giving a resolution of 0.4%. One of the applications of such monochromatic infrared sensors can be found in infrared-radiation absorption measurements where, for instance, gas concentration can be measured by tuning the sensor to a wavelength with maximum absorption by the gas. Because the Fresnel Zone Plate has an inherent amplification, the sensitivity of such sensors could be quite high.

Vacuum Sensors

A sensor to which much research has been devoted over the last few years is the integrated-thermopile vacuum sensor [19–22]. The importance of the thermal vacuum sensor is increased by the insight it gives into the thermal characteristics of micromachined thermal sensors, which are always immersed in a thermally conductive ambient. Therefore, measurements have been performed at sensors of all three structures, such as 6–9 mm long cantilever beams (see Fig. 10). Typical results are shown in Fig. 11 for a floating membrane of $3.4 \times 3.4 \text{ mm}^2$, having a sensitivity

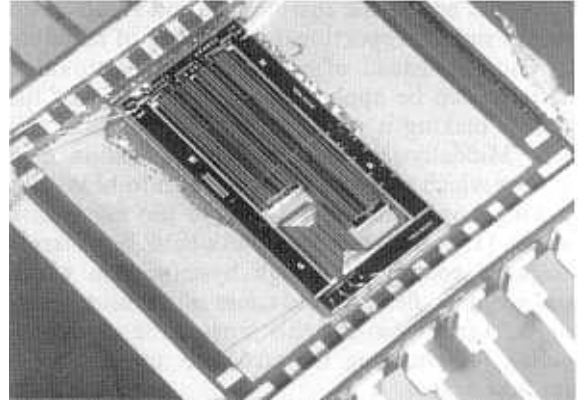


Fig. 10. Double-beam integrated thermopile vacuum sensor with beams 6.3 and 9 mm long, $10 \mu\text{m}$ thick and 1.7 mm wide.

of approximately 5%/Pa ($100\,000 \text{ Pa} = 1 \text{ atm}$). It has been found that these results agree very well both qualitatively and quantitatively with the predictions of theoretical models of vacuum sensors. As a consequence, the behavior of integrated-thermopile vacuum sensors can be described by a three-parameter model with an inaccuracy of less than 1% over an extensive pressure range, which makes (computer-calculated) corrections for temperature and gas type possible. State-of-the-art for floating-membrane integrated-thermopile vacuum sensors is presently a sensitivity of 12–15%/Pa ($\approx 2000\%/Torr$), a resolution of 1–10 μPa and a power consumption of approximately 1 mW at 100 mV zero-pressure output (offset) signal; all this for a sensor of 5–6 mm^2 .

Figure 11 also reveals the characteristics of some other integrated thermal sensors, namely that of the fluid type/mixture sensor and the fluid-level sensor. This sensor has a distinctly different output for different gas types such as

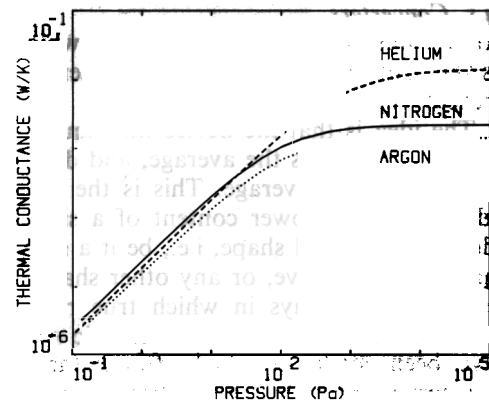


Fig. 11. Experimental results for a floating-membrane vacuum sensor of $3.4 \times 3.4 \text{ mm}^2$, dissipated power in the membrane versus gas pressure.

helium, nitrogen and argon (in fact, it is the thermal conductivity of the gas which is decisive). This indicates the possibility of detecting gas type, by observing a threshold output voltage which lies in between the output voltages of the different gases, or even the composition of a binary mixture by calibrating the sensor. Also the level detection becomes clear, because detection whether the sensor is immersed in one or the other type of fluid is the same as a gas-type detection.

Flow Sensors

The last example of integrated-thermopile sensors to be discussed here is the flow sensor. This sensor has been the object of research in Delft since 1976. At first, wafer-thick sensors were studied, which have the advantage of ruggedness, and of allowing measurement through the wall of a pipe [23]. Recently, van Oudheusden has studied the implementation of two-dimensional flow sensors in order to make wind meters. Both wafer-thick and floating-membrane sensors have been tested in this application [24, 25]. The floating-membrane wind-meter set-up is shown in Fig. 12. This sensor has the advantage that the temperature increase of the sensor with respect to the wind flow can be measured in the same chip. This is done by integrating the thermopile in the suspension beam of the floating membrane, which then measures the temperature elevation of the membrane (see Fig. 13). In sensors which are not etched, the good thermal conductivity of the silicon assures an even temperature across the entire chip, preventing the chip from measuring both the temperature elevation of the hot areas and the ambient temperature. The first measurements on etched wind meters indicate a measurement inaccuracy of less than 3° in wind angle and less than 5% in wind velocity [25].

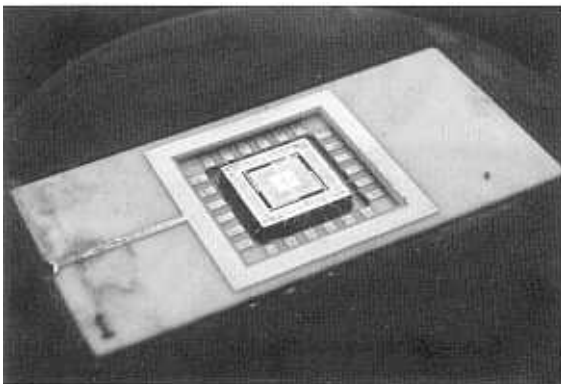


Fig. 12. Set-up of the floating-membrane wind meter for wind velocity and wind angle measurements.

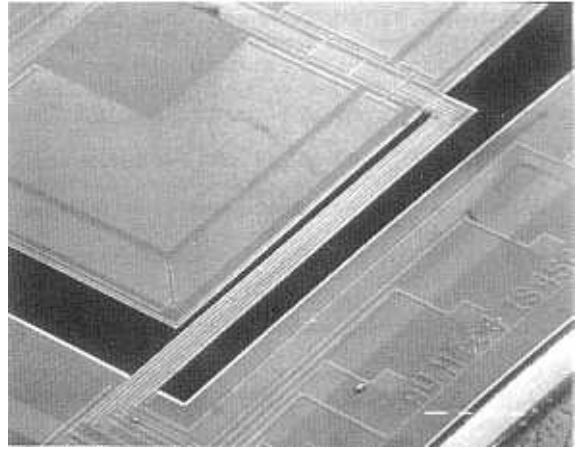


Fig. 13. SEM of one suspension beam of the floating-membrane wind meter, showing the aluminum thermopile interconnections on the beam.

Conclusions

Many of the thermal sensing principles discussed in this paper have been implemented in integrated-thermopile sensors by now. The unique characteristics of silicon, especially the excellent micromachining possibilities and the option of on-chip electronics, make these sensors very competitive. Various structures are available to tailor the thermal characteristics of the sensor to the application, and the compatibility of the thermopile and etching processes with standard integrated-circuit production processes allows on-sensor electronics to obtain an optimum electrical connection to the outside. Except for psychrometers, each of the above-mentioned sensors is predicted a glamorous future.

Acknowledgements

The authors would like to thank Professor S. Middelhoek and Dr J. H. Huijsing for their continuous guidance with the research on thermopile sensors over the past 10 years. Many of the devices discussed here have been expertly made by the staff of the Integrated Circuits Workshop of Delft University of Technology, for which we want to express our thanks explicitly. The advice from and discussions with Ir P. K. Nauta and L. Smit regarding the technology of the sensor fabrication have always been highly appreciated.

References

- 1 A. W. van Herwaarden and P. M. Sarro, Thermal sensors based on the Seebeck effect, *Sensors and Actuators*, 10 (1986) 321–346.

- 2 G. D. Nieveld, Thermopiles fabricated using silicon planar technology, *Sensors and Actuators*, 3 (1983) 179–183.
- 3 P. M. Sarro and A. W. van Herwaarden, Silicon cantilever beams fabricated by Electrochemically Controlled Etching for sensor applications, *J. Electrochem. Soc.*, 133 (1986) 1724–1729.
- 4 P. M. Sarro, H. Yashiro, A. W. van Herwaarden and S. Middelhoek, An infrared sensing array based on integrated silicon thermopiles, *Sensors and Actuators*, 14 (1988) 191–201.
- 5 B. W. van Oudheusden, Silicon flow sensors, *Proc. IEE D*, 135 (1988) 373–380.
- 6 A. W. van Herwaarden and P. M. Sarro, Performance of integrated thermopile vacuum sensors, *J. Phys. E*, 21 (1989) 1162–1167.
- 7 A. W. van Herwaarden, H. P. Hochstenbach and C. J. P. M. Harmans, Integrated true RMS converter, *IEEE Trans. Instrum. Meas.*, IM-35 (1986) 224–225.
- 8 H. N. Norton, *Sensors and Analyzer Handbook*, Prentice-Hall, Englewood Cliffs, NJ, 1982.
- 9 H. N. Norton, *Handbook of Transducers for Electronic Measuring Systems*, Prentice-Hall, Englewood Cliffs, NJ, 1969.
- 10 H. K. P. Neubert, *Instrument Transducers*, Clarendon Press, Oxford, 1975.
- 11 P. H. Mansfield, *Electrical Transducers for Industrial Measurement*, Butterworths, London, 1973.
- 12 P. H. Sydenham (ed.), *Handbook of Measurement Science*, Vol. 2, Wiley, Chichester, 1983.
- 13 S. Middelhoek, personal communication.
- 14 H. G. Kerkhoff and G. C. M. Meijer, An integrated electrothermal amplitude detector using the Seebeck effect, *Proc. ESSCIRC, Southampton, U.K., 1979*, pp. 31–33.
- 15 *Calibration Certificate 1.5.5421/6409*, Dutch National Service of Metrology, Delft, The Netherlands, 1986.
- 16 P. M. Sarro and A. W. van Herwaarden, An integrated silicon thermopile infrared detector, *Proc. 16th ESSDERC '86, Cambridge, U.K., 8–11 Sept. 1986*, pp. 99–100.
- 17 P. M. Sarro and A. W. van Herwaarden, IR detector based on an integrated silicon thermopile, *4th Int. Symp. Optics and Optoelectronics, Applications, Science and Engineering, The Hague, The Netherlands, 30 Mar.–3 Apr., 1987; Proc. SPIE 807*, pp. 113–118.
- 18 P. M. Sarro, H. Yashiro, A. W. van Herwaarden and S. Middelhoek, An integrated thermal infrared sensing array, *Sensors and Actuators*, 14 (1988) 191–201.
- 19 A. W. van Herwaarden and P. M. Sarro, Double-beam integrated thermal vacuum sensor, *J. Vac. Sci. Technol.*, A5 (4) (1987) 2454–2457.
- 20 A. W. van Herwaarden and P. M. Sarro, Integrated thermal vacuum sensor with extended range, *Vacuum*, 38 (1988) 449–453.
- 21 A. W. van Herwaarden and P. M. Sarro, Floating-membrane thermal vacuum sensor, *Sensors and Actuators*, 14 (1988) 259–268.
- 22 A. W. van Herwaarden and P. M. Sarro, Performance of integrated thermopile vacuum sensors, *J. Phys. E*, 21 (1988) 1162–1167.
- 23 B. W. van Oudheusden, Silicon flow sensors, *IEE Proc.*, 135 (1988) 373–380.
- 24 B. W. van Oudheusden and J. H. Huijsing, An electronic wind meter based on a silicon flow sensor, *Sensors and Actuators*, A21–A23 (1990) 420–424.
- 25 B. W. van Oudheusden and A. W. van Herwaarden, High-sensitivity 2-D flow sensor with an etched thermal isolation structure, *Sensors and Actuators*, A21–A23 (1990) 425–430.